

Journal of Materials Chemistry C

Accepted Manuscript



This is an *Accepted Manuscript*, which has been through the Royal Society of Chemistry peer review process and has been accepted for publication.

Accepted Manuscripts are published online shortly after acceptance, before technical editing, formatting and proof reading. Using this free service, authors can make their results available to the community, in citable form, before we publish the edited article. We will replace this *Accepted Manuscript* with the edited and formatted *Advance Article* as soon as it is available.

You can find more information about *Accepted Manuscripts* in the [Information for Authors](#).

Please note that technical editing may introduce minor changes to the text and/or graphics, which may alter content. The journal's standard [Terms & Conditions](#) and the [Ethical guidelines](#) still apply. In no event shall the Royal Society of Chemistry be held responsible for any errors or omissions in this *Accepted Manuscript* or any consequences arising from the use of any information it contains.

COMMUNICATION

The overlooked role of reduced graphene oxide in the reinforcement of hydrophilic polymers

Cite this: DOI: 10.1039/x0xx00000x

A. Flores,^a H. J. Salavagione,^b F. Ania,^a G. Martínez,^b G. Ellis^b and M. A. Gómez-Fatou^b

Received 00th January 2012,
Accepted 00th January 2012

DOI: 10.1039/x0xx00000x

www.rsc.org/

Abstract. The covalent incorporation of reduced graphene oxide to a hydrophilic polymer demonstrates that, contrary to current opinion, reinforcement can be attributed to a change in water affinity. Advanced nanoindentation techniques show that the deterioration of the mechanical properties of poly(vinyl alcohol) under high relative humidity can be avoided by incorporating a small quantity of reduced graphene oxide at molecularly-controlled locations.

Over recent years graphene has stimulated intense research, not only as a promising reinforcing filler in polymeric materials but one that can also provide electrical conductivity and/or improved thermal and barrier properties to the host matrices.¹⁻⁷ Binding strategies appear as an interesting route to develop nanocomposites with optimal morphology and properties.⁷ It is generally accepted that the effective dispersion of graphene and the interfacial interactions with the matrix are fundamental to achieve superior properties, independent of the nature of the polymer host. This reasoning has been commonly used to explain improvements in hardness, and storage or Young's moduli of both hydrophobic polymers⁸ and highly hydrophilic matrices.⁹⁻¹² However, and contrary to the case for non-polar polymers, hydrophilic polymers such as poly(vinyl alcohol) (PVA) absorb water leading to plasticization¹³ with significant consequences on modulus and hardness¹⁴ that can only be controlled through the use of additives.¹⁵ Water uptake is related to the ease of formation of polymer/water hydrogen bonding interactions, and the control of these events at a molecular-level is an essential issue for property stabilization.

Graphene oxide (GO) can be properly dispersed in water providing adequate means for its facile introduction into hydrophilic polymer matrices.^{10,11,16} Hydrogen bonding between GO and the hydrophilic polymer is believed to promote the filler-matrix interaction^{10,11} and has been found to be the driving force for the stabilization of Layer-

by-Layer (LbL) structures.¹⁷ Outstanding mechanical properties have been reported for natural biomaterial-GO LbL structures and explained as a consequence of the heterogeneity of the interface interactions.¹⁸ Graphene reinforced composites can be produced via subsequent reduction process of graphene oxide reinforced composites.^{11,19} Mechanical enhancements with the introduction of small amounts of graphene^{11,19} or graphene oxide^{10,11,16,20} to PVA have been reported using covalent⁹ and non-covalent strategies,^{10,11,16,19,20} and discussed in terms of at least one of the following issues: i) exfoliation, dispersion and/or orientation of the filler; ii) interfacial interaction with the matrix and iii) filler nucleating effect on the polymer matrix. It has been demonstrated that covalent attachment of graphene to polymers has a more significant effect on polymer properties than physical mixtures, because the filler particles become an integral part of the polymer chains.^{9,21,22} It has been previously shown for PVA that the carbonaceous filler is selectively incorporated into chain segments with stereospecific conformations, which strongly alters the nature and distribution of hydrogen bonding along the polymer chains.^{21,22} This molecular-level selectivity can be expected to change the water affinity of the hydrophilic polymer and could impart new massive properties to the material.

In the present work we analyse the effect of incorporating reduced graphene oxide (RGO), hereafter for simplicity also referred to as graphene, into PVA on the surface mechanical properties measured by nanoindentation. Covalent linking of graphene at molecular-controlled locations to PVA appears as a unique approach to modulate water uptake and stabilize the mechanical properties.

Films of PVA and RGO-PVA with 1.8 wt. % graphene content were prepared by slow evaporation from water solutions. Graphene was covalently incorporated via esterification of PVA with GO (GO-PVA), followed by reduction of the latter with hydrazine to produce a reduced graphene oxide-PVA nanocomposite, as previously reported.²¹ Although oxidative debris commonly adheres to the

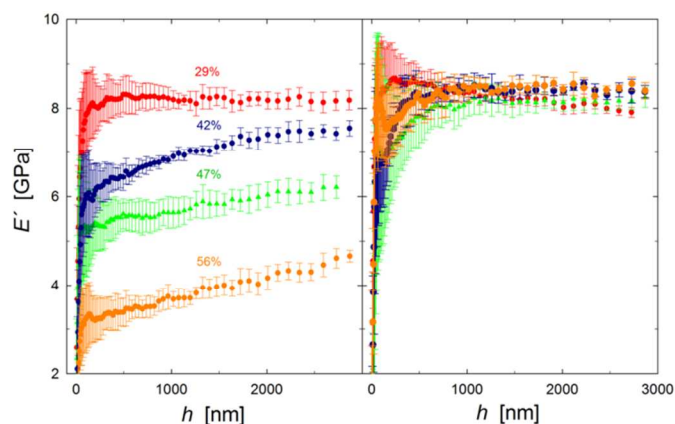


Fig. 1. Storage modulus, E' , as a function of indenter displacement into the surface, h , at different chamber relative humidity, RH, for: (left) PVA and (right) RGO-PVA. $\dot{\epsilon} = 0.05 \text{ s}^{-1}$.

GO sheets,²³⁻²⁵ in our case it is removed in the subsequent reduction steps²⁵ and esterification, and no debris was observed in the final RGO-PVA materials as shown by thermogravimetry (Fig. S1). Small fragments of PVA and PVA-RGO films were mounted vertically, embedded in epoxy and polished for nanoindentation studies, as described in the supporting information. Scanning electron microscopy images of the exposed cross section areas revealed similar surface morphology and roughness for both PVA and RGO-PVA (Fig. S2).

In agreement with preceding studies,^{14,15} it was found that the mechanical properties of PVA strongly depend on relative humidity, RH, of the test environment. In Fig. 1 (left) the indentation storage modulus E' exhibits constant values as a function of displacement of the indenter into the surface, h , for RH = 29 % corresponding to the conditions of sample storage prior to indentation measurements. The E' behaviour within the first ~ 500 nm can be disregarded because it is influenced by surface roughness and a number of material-independent effects including uncertainty in the tip area calibration.²⁶ However, for $h > 500$ nm the limited surface roughness (see Fig. S2) allows a relatively constant value of E' with h to be clearly observed. Similar indentation modulus values, in the range 7 - 8 GPa, have been reported for other solution cast PVA films.^{17,27} When the chamber humidity was increased to higher values and the materials conditioned for only a few hours before indentation testing, E' increased as the indenter penetrated towards larger deformation volumes, since the plasticizing effect of the water molecules starts at the near surface and progresses towards the bulk. The most stimulating results appear in Fig. 1 (right), where it can be observed that the E' values of RGO-PVA are unaffected by the relative humidity. Here the mechanical improvement on the incorporation of RGO is most remarkable for the highest moisture levels. Similar results were obtained for H and are available in the supporting information (Fig. S3). Additional indentation measurements at low humidity (RH = 16%), also included in the supporting information (Fig. S4), clearly back up the contention that the mechanical properties of RGO-PVA remain unaffected with RH, whilst those of PVA change noticeably. It is noteworthy from Fig. S4 that on reducing the chamber humidity, the mechanical properties of PVA immediately rise at the surface showing a decreasing trend with penetration depth. Results clearly reveal that the mechanical properties of PVA with RH are stabilized in the presence of graphene and a constant E' value is achieved at all penetration depths. While the reduced hydrophilic character of PVA-graphene nanocomposites has been proposed for pure mixtures of PVA and

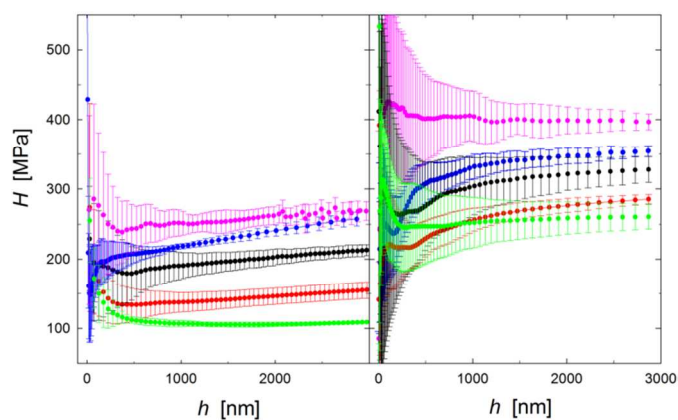


Fig. 2. Hardness, H , as a function of displacement into the surface, h , for: (left) PVA and (right) RGO-PVA, at different strain rates. From top to bottom: $\dot{\epsilon} = 0.15 \text{ s}^{-1}$, $5 \times 10^{-2} \text{ s}^{-1}$, $2.5 \times 10^{-2} \text{ s}^{-1}$, $5 \times 10^{-3} \text{ s}^{-1}$ and $5 \times 10^{-4} \text{ s}^{-1}$. RH = 42%.

graphene,^{6,28} from our observations it appears that when graphene is covalently incorporated the influence on the water uptake of the hydrophilic polymer produces a dramatic change in mechanical properties. The reduction of water uptake induced by the presence of graphene was further explored gravimetrically by quantifying the amount of absorbed water at different RH and by contact angle measurements (Table S1).

It was also found that the creep properties are significantly affected by the introduction of graphene. Fig. 2 shows the hardness variation as a function of indenter displacement for PVA and RGO-PVA at different strain rates, $\dot{\epsilon}$, and RH = 42 %. As can be anticipated, the hardness decreases with decreasing strain rate for both materials (see also Fig. S5 for results at RH = 29 %). It is noteworthy that the H values for PVA are significantly lower than those of RGO-PVA for a given $\dot{\epsilon}$ value. Most interesting is the observation that the sensitivity of PVA to strain rate is reduced when graphene is incorporated into the host matrix, as suggested by the narrower range of H values of the nanocomposite at large penetration depths (clearly observed in Fig. S6 of the supporting information illustrating a double logarithmic plot of H vs. $\dot{\epsilon}$ for RH = 29 % and 42 %). Assuming that $\dot{\epsilon} \propto H^n$, the creep exponent n at RH = 29 % is determined to be significantly larger for RGO-PVA ($n \approx 12$) than for PVA ($n \approx 9$) suggesting that the nanocomposite is less sensitive to creep than the neat polymer. Most importantly, in the case of RGO-PVA the creep resistance is unaltered when raising the RH to 42 %, whereas it is clearly deteriorated in case of PVA ($n \approx 6$). Once again, incorporation of only 1.8 wt.% of graphene to the host matrix seems to dramatically change the mechanical behaviour at ambient moisture.

Indentation tests were also performed on a GO-PVA sample with the aim of shedding some light into the mechanism of water absorption and the effect on the mechanical properties. GO is expected to exhibit a higher sensitivity to hydrogen bonding than RGO. The amount of GO in GO-PVA was identical to that of RGO in RGO-PVA (1.8 wt. %) as the latter was prepared by exposing the former to a final reduction process. Fig. 3 presents E' and H as a function of displacement for PVA, GO-PVA and RGO-PVA for two distinct RH environments (34 - 38% and 54 - 56%) with $\dot{\epsilon} = 0.05 \text{ s}^{-1}$. It is clearly seen that the mechanical properties of the host matrix and the reinforced nanocomposites are comparable at RH = 34 - 38% (at lower strain rates the differences are more notable, as shown in Fig. S6). However, as soon as RH is raised to 54 - 56%, the curves of E'

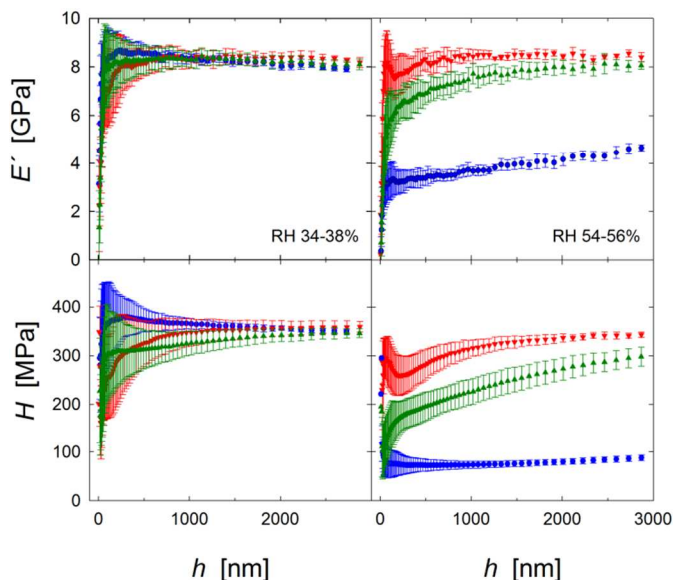


Fig. 3. E' and H as a function of h for: (●) PVA, (▼) RGO-PVA and (▲) GO-PVA at: (left) RH = 34% for PVA and RGO-PVA, RH = 38% for GO-PVA; (right) RH = 56% for PVA and RGO-PVA, RH = 54% for GO-PVA. $\dot{\epsilon} = 0.05 \text{ s}^{-1}$.

and H for the three materials can be clearly differentiated, that of GO-PVA being intermediate between those of PVA and RGO-PVA. These results clearly suggest that modification of the hydrogen bonding environment plays a fundamental role. The plasticizing effect of water disrupting hydrogen bonding in PVA is significantly hindered when GO is covalently incorporated into the matrix. The covalent attachment of GO to the polymer chains appears to hamper the formation of hydrogen bonds with water, although some groups at the GO surface may also form hydrogen bonding.

Preliminary FTIR measurements recorded from PVA and RGO-PVA under different RH conditions only showed very subtle variations in the hydrogen bonding environment, manifested in the band shape and width of the ν_{OH} (O-H stretching) region (see inset in Fig. S7a). However, some initial evidence for efficient elimination of absorbed water in samples subjected to high RH was found (see Fig. S7b). A more detailed spectroscopic study is currently underway and will be reported elsewhere.

Conclusions

Results offer a new understanding on the reinforcing effect of graphene in biocompatible hydrophilic polymers. We have demonstrated that highly hydrophobic graphene stabilizes the mechanical properties of PVA against moisture absorption. Storage modulus, hardness and creep properties of PVA remain unchanged with RH in the range 29% – 56% when a small amount of RGO (1.8 wt. %) is covalently incorporated to the polymer matrix, while those of the neat material are reduced by approximately half of the original value. The changes in the mechanical properties obtained when reinforcing PVA with graphene have to be mainly attributed to the dramatic reduction in water uptake, while the commonly invoked effective filler–matrix load transfer only seems to play a secondary role.

Acknowledgments

The authors wish to thank the MICINN (Ministerio de Ciencia e Innovación), Spain, for funding the research reported under grants FIS2010-18069, MAT2010-21070-C02-01, and MINECO MAT2013-47898-C2-1-R, MAT2013-47898-C2-2-R. HJS would like to acknowledge the MICINN for a ‘Ramón y Cajal’ Senior Research Fellowship. We are most grateful to Mr. David Gómez for his valuable help with the SEM measurements.

Notes and references

^a Departamento de Física Macromolecular, Instituto de Estructura de la Materia (IEM-CSIC), Serrano 119, 28006 Madrid, Spain.

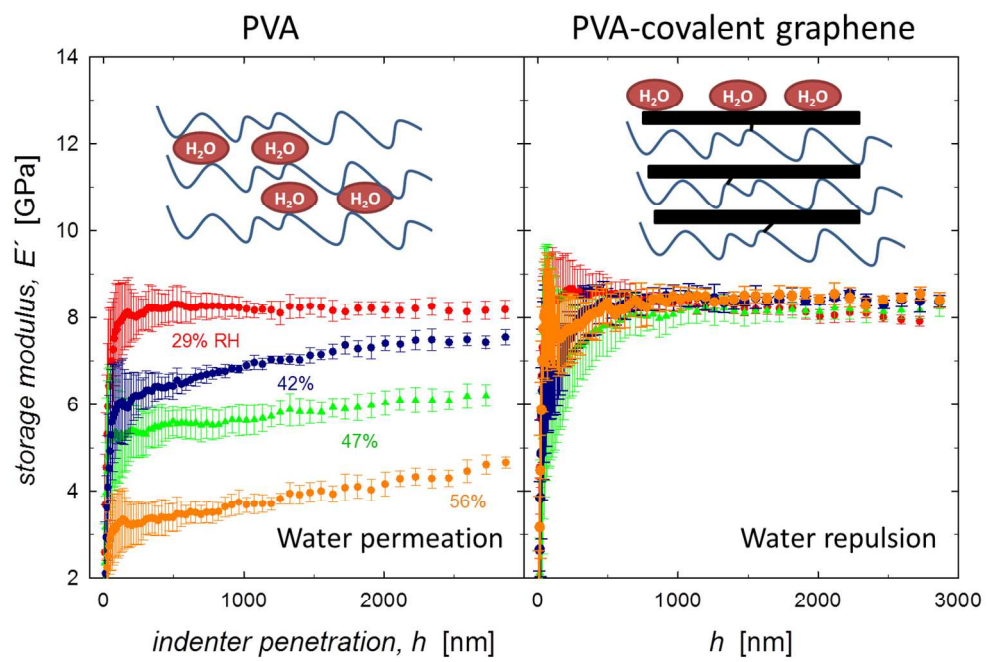
^b Departamento de Física de Polímeros, Elastómeros y Aplicaciones Energéticas, Instituto de Ciencia y Tecnología de Polímeros (ICTP-CSIC), Juan de la Cierva 3, 28006 Madrid, Spain.

Electronic Supplementary Information (ESI) available: [Full experimental details; variation of hardness, H , with different parameters; vibrational and XRD characterization of samples.]. See DOI: 10.1039/c000000x/

1. T. Ramanathan, A. A. Abdala, S. Stankovich, D. A. Dikin, M. Herrera Alonso, R. D. Piner, D. H. Adamson, H. C. Schniepp, X. Chen, R. S. Ruoff, S. T. Nguyen, I. A. Aksay, R. K. Prud'Homme, L. C. Brinson, *Nat. Nanotechnol.*, 2008, **3**, 327–331.
2. J. R. Potts, D. R. Dreyer, C. W. Bielawski, R. S. Ruoff, *Polymer*, 2011, **52**, 5–25.
3. H. J. Salavagione, G. Martínez, G. Ellis, *Macromol. Rapid Commun.*, 2011, **32**, 1771–1789.
4. Y. Zhu, S. Murali, W. Cai, X. Li, J. W. Suk, J. R. Potts, R. S. Ruoff, *Adv. Mater.*, 2010, **22**, 3906–3924.
5. C. Xiang, P. J. Cox, A. Kukovec, B. Genorio, D. P. Hashim, Z. Yan, Z. Peng, C. C. Hwang, G. Ruan, E. L. G. Samuel, P. M. Sudeep, Z. Konya, X. R. Vajtai, P. M. Ajayan, J. M. Tour, *ACS Nano*, 2013, **7**, 10380–10386.
6. H. D. Huang, P. G. Ren, J. Chen, Q. W. Zhang, X. Ji, Z. M. Li, *J. Membr. Sci.*, 2012, **409-410**, 156–163.
7. K. Hu, D. D. Kulkarni, I. Choi, V. V. Tsukruk, *Prog. Polym. Sci.*, 2014, **39**, 1934–1972.
8. S. Stankovich, D. A. Dikin, G. H. B. Dommett, K. M. Kohlhaas, E. J. Zimney, E. A. Stach, R. D. Piner, S. T. Nguyen, R. S. Ruoff, *Nature*, 2006, **442**, 282–286.
9. M. Cano, U. Khan, T. Sainsbury, A. O'Neill, Z. Wang, I. T. McGovern, W. K. Maser, A. M. Benito, J. N. Coleman, *Carbon*, 2013, **52**, 363–371.
10. J. Liang, Y. Huang, L. Zhang, Y. Wang, Y. Ma, T. Guo, Y. Chen, *Adv. Funct. Mater.*, 2009, **19**, 2297–2302.
11. C. Bao, Y. Guo, L. Song, Y. Hu, *J. Mater. Chem.*, 2011, **21**, 13942–13950.
12. L. Liu, Y. Gao, Q. Liu, J. Kuang, D. Zhou, S. Ju, B. Han, Z. Zhang, *Small*, 2013, **9**, 2466–2472.
13. J. C. Grunlan, A. Grigorian, C. B. Hamilton, A. R. Mehrabi, *J. Appl. Polym. Sci.*, 2004, **93**, 1102–1109.

14. X. Qi, X. Yao, S. Deng, T. Zhou, Q. Fu, *J. Mater. Chem., A* 2014, **2**, 2240–2249.
15. M. S. Peresin, Y. Habibi, A. H. Vesterinen, O. J. Rojas, J. J. Pawlak, J. V. Seppälä, *Biomacromolecules*, 2010, **11**, 2471–2477.
16. Y. Xu, W. Hong, H. Bai, C. Li, G. Shi, *Carbon*, 2009, **47**, 3538–3543.
17. X. Zhao, Q. Zhang, Y. Hao, Y. Li, Y. Fang, D. Chen, *Macromolecules*, 2010, **43**, 9411–9416.
18. K. Hu, M. K. Gupta, D. D. Kulkarni, V. V. Tsukruk, *Adv. Mater.*, 2013, **25**, 2301–2307.
19. X. Zhao, Q. Zhang, D. Chen, *Macromolecules* 2010, **43**, 2357–2363.
20. K. E. Prasad, B. Das, U. Maitra, U. Ramamurty, C. N. R. Rao, *Proc. Natl. Acad. Sci.*, 2009, **10**, 13186–13189.
21. H. J. Salavagione, M. A. Gómez, G. Martínez, *Macromolecules*, 2009, **42**, 6331–6334.
22. H. J. Salavagione, M. A. Gómez, G. Martínez, *J. Mater. Chem.*, 2009, **19**, 5027–5032.
23. J. P. Rourke, P. A. Pandey, J. J. Moore, M. Bates, I. A. Kinloch, R. J. Young, N. R. Wilson, *Angew. Chem. Int. Ed.*, 2011, **50**, 3173–3177.
24. V. R. Coluci, D. S. T. Martinez, J. G. Honório, A. F. de Faria, D. A. Morales, M. S. Skaf, O. L. Alves, G. A. Umbuzeiro, *J. Phys. Chem. C.*, 2014, **118**, 2187–2193.
25. H. R. Thomas, S. P. Day, W. E. Woodruff, C. Vallés, R. J. Young, I. A. Kinloch, G. W. Morley, J. V. Hanna, N. R. Wilson, J. P. Rourke, *Chem. Mater.*, 2013, **25**, 3580–3588.
26. A. M. Diez-Pascual, M. A. Gómez-Fatou, F. Ania, A. Flores, *Prog. Mater. Sci.*, 2015, **67**, 1–94.
27. M. Cadek, J. N. Coleman, V. Barron, *Appl. Phys. Lett.*, 2002, **81**, 5123–5125.
28. J. Wang, X. Wang, C. Xu, M. Zhang, X. Shang, *Polym. Int.*, 2011, **60**, 816–822.

Mechanical properties of PVA are stabilized against moisture absorption by highly hydrophobic graphene.



TOC